

Strain in GaAs by low-dose ion implantation

B. M. Paine,^{a)} N. N. Hurvitz,^{b)} and V. S. Speriosu^{c)}

Electrical Engineering 116-81, California Institute of Technology, Pasadena, California 91125

(Received 2 June 1986; accepted for publication 10 October 1986)

The production of strain in (100) GaAs by low-dose ion implantation has been investigated. Implantations were conducted at room temperature with ions of He, B, C, Ne, Si, P, and Te. Energies were between 100 and 500 keV, and each species was implanted over a range of doses sufficient to create perpendicular strain below 0.3%. The perpendicular strains ϵ^\perp were measured by x-ray double-crystal diffractometry about the (400) Bragg condition. Detailed depth profiles of ϵ^\perp were obtained by fitting the resulting rocking curves with a kinematic model for the diffraction. For all implantations the maximum in the ϵ^\perp distribution was found approximately from the separation of the lowest-angle prominent oscillation from the substrate peak. The depth profiles of perpendicular strain had the same shape as the calculated profiles of energy deposited per ion by nuclear collisions, F_D . The maximum perpendicular strains scaled linearly with the dose ϕ of the implanted ions for all ion species. Also the ratio of maximum strain to dose was found to vary linearly with F_D over more than 2 orders of magnitude in F_D . We therefore conclude that $\epsilon^\perp = K\phi F_D$ at all depths, where K is a constant. The value of K was found to be $(5 \pm 1) \times 10^{-2} \text{ \AA}^3/\text{eV}$. Our results suggest that this holds for any ion species in the mass range 4–128 amu, with energy in the hundreds of keV, implanted into (100) GaAs at room temperature, provided the maximum strain is less than 0.3%.

INTRODUCTION

Low-dose implantation of dopant atoms is an important part of the preparation of many GaAs devices. X-ray double-crystal diffractometry (DCD) measurements have shown that the implantation process creates crystal strain in GaAs,¹⁻⁴ as well as other materials (see, e.g., Refs. 1 and 5–8). The strain is positive and perpendicular to the sample surfaces, and occurs only in the material penetrated by the energetic ions. The profile of strain with depth can be calculated from the x-ray data. In magnetic garnet, implantation of several species, with energies of 60–200 keV, causes strain profiles which scale with dose and closely follow the profiles of energy deposited per ion in atomic displacements.⁷ Similar results have been found for implantation in Si.^{8,9} Thus it appears that strain is proportional to the density of energy deposited by nuclear interactions. In GaAs, strain profiles have been reported only for MeV implantations.¹⁰ However, Speriosu *et al.*¹ have reported DCD measurements of the peak perpendicular strains, $\epsilon_{\text{max}}^\perp$, as a function of dose for room-temperature implantation of 230–300-keV Si⁺ ions in GaAs, as well as Ge and Si. They found that for Ge and Si, $\epsilon_{\text{max}}^\perp$ varies linearly with dose from low damage levels up to amorphicity. For GaAs, $\epsilon_{\text{max}}^\perp$ increases monotonically with dose for low doses, but saturates above about 5×10^{13} ions/cm². Thus, the strain in GaAs is clearly not a linear function of nuclear energy deposition at all doses. In this paper we describe a detailed investigation of strain in implanted GaAs in the low-dose regime, i.e., below the saturation level. In particular, we have studied the dependence on irradiation

dose and ion species and the correlation of the measured profile of strain with the calculated profile of energy deposited in nuclear interactions. We will report on the behavior of the strains above the saturation threshold in another paper.¹¹

PROCEDURE

GaAs wafers of (100) orientation were cleaved into 0.5-cm square samples, cleaned organically, and etched in a dilute solution of H₂SO₄ and H₂O₂ in water. They were mounted for implantation with the {011} planes (identified from the cleavage directions) misoriented from horizontal by about 10° and with their surface normals lying in the horizontal plane, but rotated away from the direction of incident beam by 7°. This arrangement was designed to minimize axial or planar channeling of the implanted ions. Thermal conducting paste was placed between the samples and the holder and beam currents were kept below 0.2 $\mu\text{A}/\text{cm}^2$, so as to maintain the implanted material as close as possible to room temperature. The samples were implanted over their entire area with ions of He, B, C, Ne, Si, P, and Te. Energies were 100, 240, and 500 keV for the He, C, and Te ions, respectively, and 300 keV for the others. These energies were selected to give roughly the same projected ranges [$\sim (3-4) \times 10^3 \text{ \AA}$]. Before conducting the Si implantation, a careful spectrum of all species emanating from the accelerator was recorded and checked for ions with a mass-to-charge ratio of 16. Singly charged molecules of ¹⁴N₂ resulting from a leak or residual air in the ion source cannot be distinguished from ²⁸Si⁺. However, absence of ions with $m/q = 16$ implies that no ¹⁶O is present, making N contamination very unlikely. Implantations of Si⁺ were only conducted when the beam of ions with $m/q = 16$ was negligible compared to all other species.

The samples were analyzed by Bragg-case x-ray double-crystal diffractometry. A sealed tube with iron target was

^{a)} Present address: Torrance Research Center, Hughes Aircraft Company, Torrance, CA 90509-2940.

^{b)} Present address: Department of Electrical Engineering and Computer Science, University of California at San Diego, La Jolla, CA 92093-0001.

^{c)} Present address: IBM Almaden Research Center, San Jose, CA 95120-6099.

used, with a first crystal of (100) GaAs with high crystalline perfection. Fe x-ray radiation was subject to a (400) diffraction in the first crystal and a monochromatic, collimated $FeK\alpha_1$ beam was selected with a pair of slits. This beam impinged on the sample where the illuminated area was always kept to less than $1 \times 1 \text{ mm}^2$. The divergence of the beam was always less than 2×10^{-3} deg. The ratio of intensity of radiation diffracted by the sample to incident intensity was measured as a function of rocking angle about the (400) Bragg condition with the $+/-$ nondispersive geometry.

The distributions of perpendicular strain as a function of depth, denoted $\epsilon^\perp(x)$, were deduced for selected samples by iterative fitting of their rocking curves with the technique of Ref. 12. In this approach, the strained material is modeled as a series of laminae, each with a perpendicular strain ϵ_j^\perp and "damage," assumed uniform in the lamina. "Damage" is random displacements of atoms from their lattice sites. This was taken to have the form of a spherically symmetric Gaussian function, with standard deviation U_j . Experience has shown that U varies approximately linearly with strain created by implantation.^{1,7,12} For GaAs, the best fits to rocking curves are obtained with $U_j = 0.35 \epsilon_j^\perp$, where ϵ^\perp has units of percent and U is in \AA . Errors in the constant of proportionality or deviations from linearity will not have a large effect on the results because at these low damage levels the rocking curves are much more sensitive to strain than to damage. The calculated rocking curves were convolved with a Gaussian function to account for the divergence of the incident beam or slight lateral nonuniformities in the sample. The width used was typically 3×10^{-3} deg.

To correlate strain with the parameters of the implantation, we have calculated the profile $F_D(x)$. This is the energy per incident ion, per unit depth, deposited at depth x in nuclear interactions. Thus $F_D(x)$ includes the energy deposited at depth x not only by the incident ion, but also by all the atoms set in motion by the collision cascade. Calculations were made by two methods, both treating GaAs as a fictional element with $Z = 32$, $A = 72.32$, and mass density equal to that of GaAs. Winterbon has tabulated the first four moments of the F_D distributions for a series of ion-to-target mass ratios.¹³ We interpolated these for all of the implantation conditions used and generated the appropriate Pearson distributions.¹⁴ The values of F_D at the peaks of the distributions were obtained from these. For conducting detailed comparisons of the exact shapes of profiles, we used the more accurate Monte Carlo simulation TRIM developed by Bierack and Haggmark.¹⁵ It was run for just two implantations (Ne and Si) for 10 000 simulated cascades each.

RESULTS AND DISCUSSION

The dashed line in Fig. 1(a) shows the experimental rocking curve for a 300-keV Si implantation at a dose of 1×10^{13} ions/cm², i.e., just below the saturation regime. The structure arising from the implantation-induced strain is clear at negative $\Delta\theta$, together with the large substrate peak at $\Delta\theta = 0$. Detailed fitting was conducted for Ne, Si, P, and Te implantations, each with several doses, from the lowest which yielded resolvable structure, up to the onset of saturation. The solid curve in Fig. 1(a) shows a typical fit. Here the

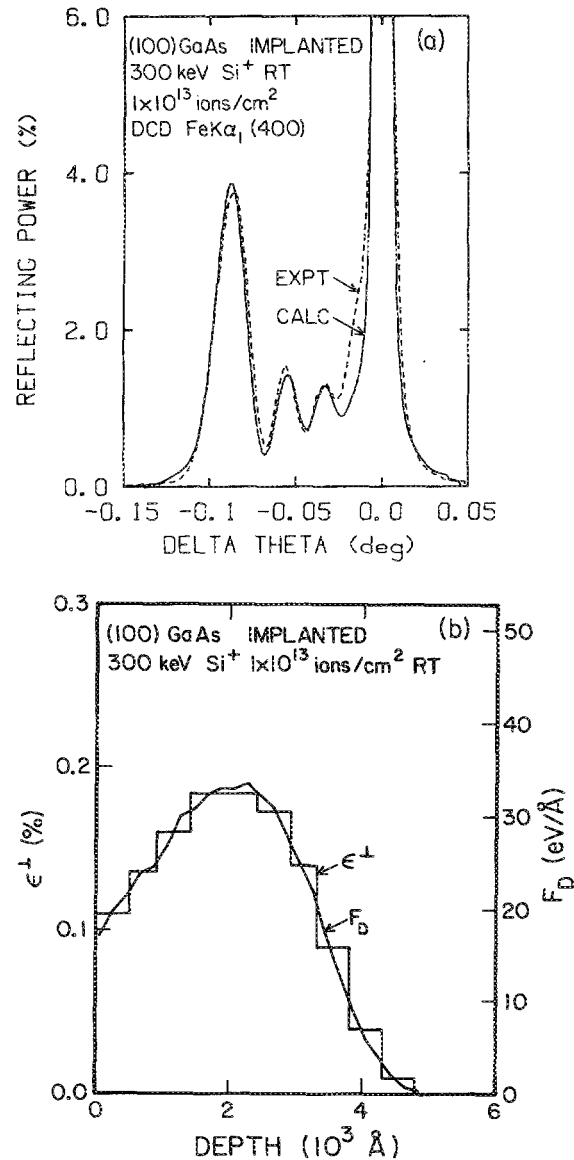


FIG. 1. (a) X-ray double-crystal diffraction rocking curves for GaAs implanted with Si ions to a low dose, i.e., generating perpendicular strain ϵ^\perp less than 0.3%. The calculated fit was generated with the $\epsilon^\perp(x)$ curve of Fig. 2. (b) Depth distribution of perpendicular strain $\epsilon^\perp(x)$, used for the calculated rocking curve in Fig. 1, together with the profile of energy deposited per incident ion by nuclear collisions, F_D .

width of the Gaussian convolution was 4.4×10^{-3} deg. The fit is good, except for a small discrepancy just below the substrate peak. This corresponds to very small strains ($\sim 0.03\%$) and may arise from the separate treatment of the strained layer and the perfect crystal substrate in this model.¹²

The profile of strain used to generate the fit of Fig. 1(a) is shown as the stepped curve in Fig. 1(b). The fits for lower doses yielded strain profiles with the same shape to within the precision of the analyses, but with magnitudes reduced by the ratios of doses. The other curve in Fig. 1(b) is the profile of F_D from the TRIM calculation, scaled vertically for easy comparison with the strain curve. It is not completely smooth because of the statistical nature of the Monte Carlo calculation. The two curves are in excellent agreement, sug-

gesting a direct connection between atomic displacements in GaAs and the formation of strain. The profile of implanted Si atoms was calculated from the Winterbon tables¹³ to have a maximum at 2950 Å—well below the peak of the ϵ^\perp curve (1800–2200 Å). Thus, we observe no contribution to the strain from the presence of the Si atoms (9×10^{-4} at. % maximum concentration). Similar good agreement was evident between the ϵ^\perp profile found by fitting and the F_D curve calculated with the TRIM code for the Ne implantation.

Figure 2 shows the experimental rocking curves recorded for a series of Si doses from 0 to 1×10^{13} ions/cm². To characterize the behavior of the strain with implantation dose we have measured the maxima of the ϵ^\perp distributions. These may be found from fitting, but a consistent and less tedious approach is to deduce them directly from the rocking curve by the relation

$$\epsilon^\perp_{\max} = -\cot \theta_B \Delta\theta_0, \quad (1)$$

where θ_B is the Bragg angle and $\Delta\theta_0$ is the angular separation of the peak of the furthest prominent oscillation from the substrate peak. In Fig. 1, the values found by fitting and direct measurement were 0.18% and 0.16%, respectively. The error in the direct measurement is small, and comparisons with several other fits showed the correction factor is essentially constant for all doses considered here.

Figure 3 shows the maximum strain found in this manner, plotted against implantation dose for all of the Si implantations up to 1×10^{13} ions/cm². Where error bars are not drawn, the uncertainties are approximately the size of the symbols. The relationship is clearly linear in this low-dose regime.

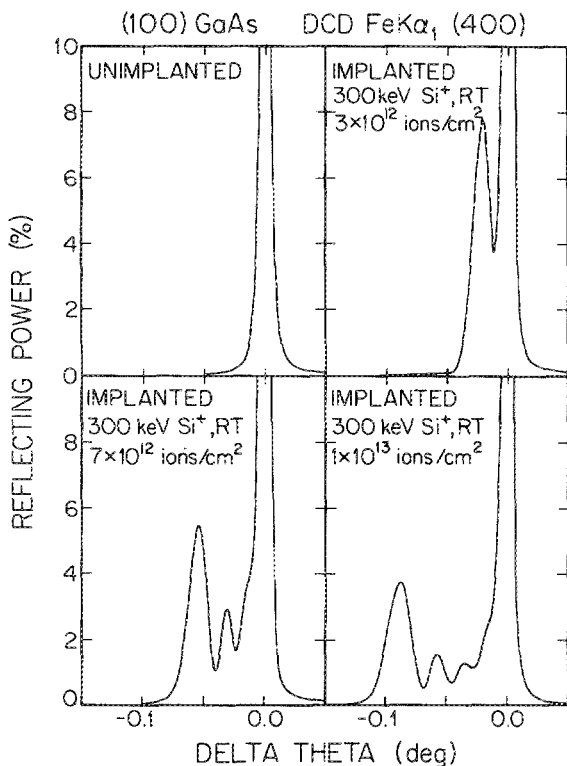


FIG. 2. Experimental rocking curves for a series of implantation doses below saturation.

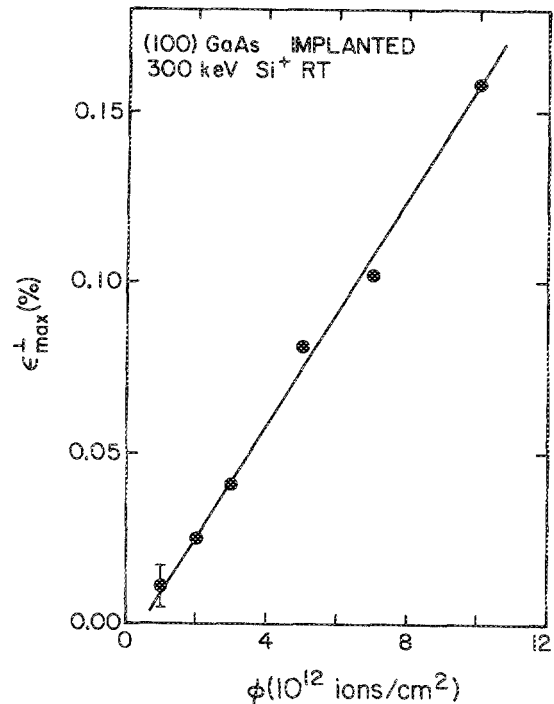


FIG. 3. Maximum perpendicular strain, measured in Si-implanted GaAs, plotted against implantation dose.

The gradient of the plot in Fig. 3 gives a measure of the rate of generation of strain, $\epsilon^\perp_{\max}/\phi$. One would expect this rate to depend on the damage energy F_D . To test this over a wide range of F_D , a similar dose dependence curve was measured for a variety of other ion species. It was assumed that for each of these the maximum strain occurs at maximum F_D , as was observed for Ne, Si, P, and Te. The maximum of F_D was found from the tables of Ref. 13. The rates of strain production are plotted against $F_{D\max}$ in Fig. 4. Here again the uncertainties of the points are of the order of the sizes of the symbols. The solid line in the figure is a least-squares fit, which is consistent with all of the data, to within the experimental uncertainties. The fit corresponds to a power-law dependence of $\epsilon^\perp_{\max}/\phi$ on $F_{D\max}$ where the power was found to be 1.1 ± 0.1 . Thus, our data are consistent with a linear dependence of $\epsilon^\perp_{\max}/\phi$ on $F_{D\max}$ over more than 2 orders of magnitude.

Assuming the relationship is in fact linear, we find $\epsilon^\perp_{\max}/\phi = (5.41F_{D\max} - 6.37) \times 10^{-3}\%$, with ϕ in units of 10^{13} ions/cm² and F_D in eV/Å. The zero offset, which is very small ($6 \times 10^{-3}\%$ strain) reflects the fact that ϵ^\perp_{\max} found from the position of the lowest-angle oscillation in the rocking curve is a slight underestimate. Since this correction is smaller than the uncertainties of most measurements, we will neglect it. We have already shown that ϵ^\perp is proportional to F_D at all depths and the shapes of the $\epsilon^\perp(x)$ profiles do not vary with dose. Therefore it follows that

$$\epsilon^\perp(x) = K\phi F_D(x) \quad (2)$$

at all depths, where K is a constant, equal to $(5 \pm 1) \times 10^{-2}$ Å³/eV. In other words, at low doses, the perpendicular strain caused by implantation in GaAs depends only on the density of energy deposited in nuclear collisions. Our results

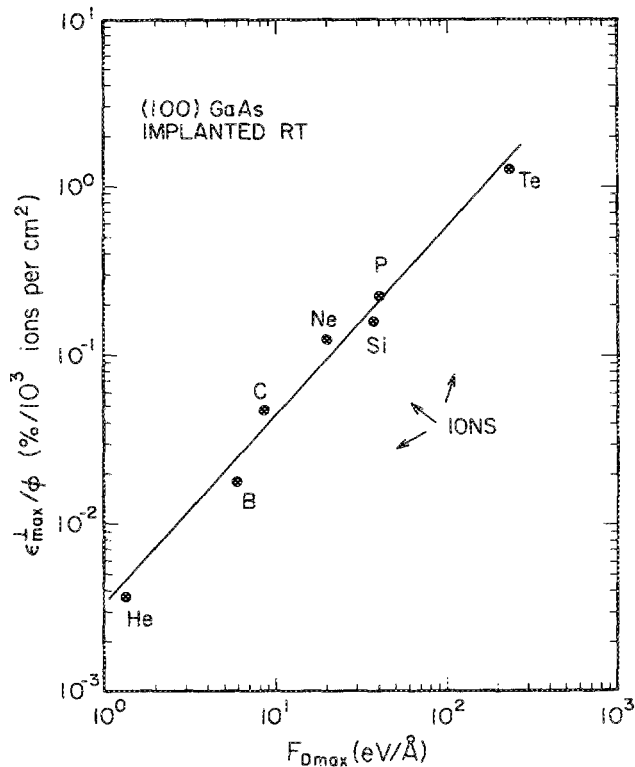


FIG. 4. Maximum perpendicular strain per unit dose, plotted against energy deposited by an ion in nuclear collisions, per unit depth.

suggest that this holds true for any ion species in the mass range 4–128 amu, with energy of several hundred keV, independent of the precise energy or identity of the ions or the depth to which they penetrate. The strain is not correlated with energy deposited by electronic stopping, or with the presence of the implanted atoms (up to concentrations of 9×10^{-4} at. %).

The value of the constant K depends on how energy deposited in the crystal lattice is converted to strain. To gain some initial insight into the physical mechanism for this process, we consider how K varies between different materials. Values can be found for Si, Ge, and magnetic garnet from earlier studies,^{1,7} assuming that K is also a universal constant in each of these media, independent of the specific parameters of the implantations. These are listed in Table I. They vary by a factor of 14 between Si and GaAs. Assuming strain is associated with displacement of atoms, material-dependent factors governing its production would include (a) the atomic densities, (b) the energy required to displace atoms, (c) defect motion, trapping, and recombination, and (d)

TABLE I. Constants K and other parameters.

Material	Crystal orientation	K ($10^{-3} \text{ \AA}^3/\text{eV}$)	N ($10^{-2} \text{ at./\AA}^3$)	E_d (eV)	$\frac{1+\nu}{1-\nu}$
Si	(100)	3.1	5.0	14	1.77
garnet	(111)	16	8.4	...	1.85
Ge	(100)	42	4.4	15	1.75
GaAs	(100)	54	4.4	...	1.90

elastic properties. The elastic properties are important because they govern how much perpendicular strain will develop, given the fact that the thick substrate prevents expansion in lateral directions. The observed strain is equal to the intrinsic strain that would develop if a thin implanted layer were standing free, multiplied by $(1 + \nu)/(1 - \nu)$, where ν is Poisson's ratio. The values of this function¹⁶ are listed in Table I; it varies by no more than 10% between these four materials. Minimum energies required to displace atoms, E_d , have been measured for many elemental materials and are tabulated in Ref. 17. These, as well as the atomic densities N are essentially the same for Si and GaAs (see Table I) and are therefore probably not responsible for the large difference in K . Consequently, it appears that defect motion, trapping, or recombination mechanisms are the most responsible for the variations of K between materials.

In conclusion, we suggest that the linear relationship between ϵ^\perp and ϕF_D could be used for routine DCD monitoring of low-dose room-temperature implantations in GaAs. The conventional alternative techniques are either destructive or involve monitoring of activated implants only. A measurement would involve recording a single (400) rocking curve like those in Fig. 2, finding $\epsilon_{\text{max}}^\perp$ by Eq. (1), and deducing the dose from Eq. (2). In this equation, $F_{D_{\text{max}}}$ can be found by interpolation of Winterbon's tables¹³ or by a simulation calculation. For accuracies of the order of a few percent, one could find $K F_{D_{\text{max}}}$ from one or more measurements of $\epsilon_{\text{max}}^\perp$ with known doses, as in Fig. 3. While the upper dose limit is that sufficient to give $\epsilon_{\text{max}}^\perp = 0.3\%$, the technique is sensitive to very low doses. For example, we have demonstrated that it has reasonable accuracy for doses down to 2×10^{12} ions/cm² for 300-keV Si and 6×10^{11} ions/cm² for 500-keV Te.

ACKNOWLEDGMENTS

We are grateful to R. S. Averback and L. J. Thompson at Argonne National Laboratory for running the TRIM calculation. We also thank M-A. Nicolet of Caltech and P. M. Asbeck of Rockwell International for their interest and encouragement. This work was supported financially by the Defense Advanced Research Projects Agency (Grant No. MDA 903-82-C-0348) and the National Science Foundation Materials Research Program (Grant No. DMR-8421119). One of us (N.N.H.) acknowledges the support of Caltech's Summer Undergraduate Research Fellowship program.

¹V. S. Speriosu, B. M. Paine, M-A. Nicolet, and H. L. Glass, *Appl. Phys. Lett.* **40**, 604 (1982).

²M. V. Prilepskii, I. M. Sukhodreva, and L. D. Cheryukanova, *Sov. Phys. Tech. Phys.* **27**, 384 (1982).

³G. F. Kalugina, F. N. Komaleeva, V. N. Mordkovich, I. M. Sukhodreva, and E. M. Temper, *Sov. Phys. Semicond.* **16**, 230 (1982).

⁴C. R. Wie, T. Vreeland, Jr., and T. A. Tombrello, *Mater. Res. Soc. Symp. Proc.* **35**, 305 (1985).

⁵B. C. Larson, C. W. White, and B. R. Appleton, *Appl. Phys. Lett.* **32**, 801 (1978).

⁶R. N. Kyutt, P. V. Petrashen, and L. M. Sorokin, *Phys. Status Solidi A* **60**, 381 (1980).

⁷B. E. MacNeal and V. S. Speriosu, *J. Appl. Phys.* **52**, 3935 (1981).

- ⁸F. Cembali, A. M. Mazzone, and M. Servidori, *Phys. Status Solidi A* **91**, K125 (1985).
- ⁹V. D. Tkachev, G. Holzer, and A. R. Chelyadinskii, *Phys. Status Solidi A* **85**, K43 (1984).
- ¹⁰C. R. Wie, T. A. Tombrello, and T. Vreeland, Jr., *Phys. Rev. B* **33**, 4083 (1986).
- ¹¹B. M. Paine and V. S. Speriosu (submitted to *J. Appl. Phys.*).
- ¹²V. S. Speriosu, *J. Appl. Phys.* **52**, 6094 (1981).
- ¹³K. B. Winterbon, *Ion Implantation Range and Energy Deposition Distributions* (Plenum, New York, 1975), Vol. 2.
- ¹⁴K. B. Winterbon, *Appl. Phys. Lett.* **42**, 205 (1983).
- ¹⁵J. P. Biersack and L. G. Haggmark, *Nucl. Instrum. Methods* **174**, 257 (1980).
- ¹⁶A. Segmüller and M. Murakami, in *Analytical Techniques for Thin Films*, edited by K. N. Tu and R. Rosenberg (Academic, New York, 1986).
- ¹⁷H. H. Anderson, *Appl. Phys.* **18**, 131 (1979).